1-2010

Multiresolution Inverse Wavelet Reconstruction from a Fourier Partial Sum

Nataniel Greene
CUNY Kingsborough Community College

JOURNAL OF CONCRETE AND APPLICABLE MATHEMATICS, VOL.8, NO.2, 353-370, 2010, COPYRIGHT 2010 EUDOXUS PRESS, LLC

Multiresolution Inverse Wavelet Reconstruction from a Fourier Partial Sum

Nataniel Greene
Department of Mathematics and Computer Science
Kingsborough Community College, CUNY
2001 Oriental Boulevard, Brooklyn, NY 11235
email: ngreene.math@gmail.com

March 16, 2009

The Gibbs phenomenon refers to the lack of uniform convergence which occurs in many orthogonal basis approximations to piecewise smooth functions. This lack of uniform convergence manifests itself in spurious oscillations near the points of discontinuity and a low order of convergence away from the discontinuities. In previous work [11,12] we described a numerical procedure for overcoming the Gibbs phenomenon called the Inverse Wavelet Reconstruction method (IWR). The method takes the Fourier coefficients of an oscillatory partial sum and uses them to construct the wavelet coefficients of a non-oscillatory wavelet series. However, we only described the method standard wavelet series and not for the continuous wavelet transform. We also only described the method for so-called *crude wavelets*: wavelets which do not admit a scaling function, and therefore lack a multiresolution analysis. Here we describe a version of IWR based on a quadrature discretization of the continuous inverse wavelet transform. We also describe the multiresolution potential of the Inverse wavelet reconstruction method, which is the ability to decompose a function into a coarse trend plus finer details.

Key Words: Gibbs phenomenon, Fourier Series, Inverse polynomial reconstruction, Wavelets, Inverse wavelet reconstruction.

1 Introduction

Fourier and orthogonal polynomial series are known for their highly accurate expansions for smooth functions. In fact it is known that the more derivatives a function has, the faster the approximation will converge. However, when a function possesses jump-discontinuities the approximation will fail to converge uniformly. In addition, spurious oscillations will cause a loss of accuracy throughout the entire domain. This lack of uniform convergence is

known as the Gibbs phenomenon. Methods for post-processing approximations which suffer from the Gibbs phenomenon include the Gegenbauer reconstruction method of Gottlieb and Shu [7, 9], the method of Pade approximants due to Driscoll and Fornberg [2], the method of spectral mollifiers due to Gottlieb and Tadmor [8] and Tadmor and Tanner [21, 22], the Inverse polynomial reconstruction (IPR) method of Shizgal and Jung [14,15,16,19,20], and the Freund polynomial reconstruction method of Gelb and Tanner [6]. These reconstruction methods can be combined with an effective method for edge-detection developed by Gelb and Tadmor [3, 4, 5], to yield an exponentially accurate reconstruction of the original function. In previous work we described a numerical method for overcoming the Gibbs phenomenon following the work of Shizgal and Jung, called the Inverse Wavelet Reconstruction method (IWR) [10,11,12]. The IWR method was shown numerically to perform at least as well as inverse polynomial reconstruction.

However, our main justification for choosing wavelets over other orthogonal or non-orthogonal bases, lies in ability of wavelets to decompose a function into a coarse trend and finer details. This decomposition is essentially what is known as a multiresolution analysis. Our previous papers on the IWR method focused on so-called *crude wavelets*: wavelets which do not admit a scaling function and which therefore do not offer a multiresolution analysis The present paper addresses the notion of multiresolution reconstruction from a Fourier partial sum. Our previous papers described the method using standard wavelet series approximations. The present paper also addresses how the method can be implemented using the continuous wavelet transform (CWT). The CWT is truncated and discretized using a uniform Trapezoidal rule or a Gauss quadrature grid and a non-standard wavelet series approximation is obtained.

We begin with a brief review of the essential definitions of wavelets which we will need. Recall that a wavelet is a function $\psi \in L^2(\mathbf{R})$ satisfying:

$$\int_{-\infty}^{\infty} \psi(x)\, dx = 0 \tag{1}$$

and

$$\int_{-\infty}^{\infty} \frac{|\Psi(\xi)|}{|\xi|} d\xi < \infty, \tag{2}$$

where Ψ here is the Fourier transform of ψ. To avoid a conflict of notations we will use a capital letter for the Fourier transform and a hat above the letter for a Fourier coefficient. The function ψ is known as a mother wavelet or an analyzing wavelet since any function $f \in L^2(\mathbf{R})$ can be expressed as a continuous sum of translations and dilations involving ψ according to the continuous wavelet transform. The continuous wavelet transform (CWT) is given by

$$F_\psi(b,a) = |a|^{-1/2} \int_{-\infty}^{\infty} f(x)\, \overline{\psi\left(\frac{x-b}{a}\right)} dx$$

and the inverse CWT is given by

$$f(x) = \frac{1}{C_\psi} \int_{-\infty}^{\infty} \int_{-\infty}^{\infty} \frac{F_\psi(b,a)}{a^2} \psi_{b,a}(x)\, dadb \tag{3}$$

where

$$\psi_{b,a}(x) = |a|^{-1/2} \overline{\psi\left(\frac{x-b}{a}\right)}$$

and

$$C_\psi = \int_{-\infty}^{\infty} \frac{|\Psi(\xi)|}{|\xi|} d\xi.$$

A discrete wavelet series is given for fixed constants a_0, b_0 by

$$f(x) = \sum_{m=-\infty}^{\infty} \sum_{l=-\infty}^{\infty} d_{m,l} \psi_{m,l}(x) \tag{4}$$

where the discrete wavelet series coefficients are given by

$$d_{m,l} = F_\psi\left(\frac{b_0 l}{a_0^m}, \frac{1}{a_0^m}\right)$$

and $\psi_{m,l}(x)$ in this case has a slightly different meaning:

$$\psi_{m,l}(x) = a_0^{m/2} \psi\left(a_0^m x - b_0 l\right).$$

In general the wavelet functions $\psi_{m,l}$ do not constitute an orthonormal basis. Instead they constitute what is known as a frame. The family of functions $\psi_{m,l}$ is a frame if

$$A\|f\|^2 \leq \sum_{m=-\infty}^{\infty} \sum_{l=-\infty}^{\infty} \left|\langle f, \psi_{m,l}\rangle\right| \leq B\|f\|^2$$

for positive constants A and B. When $A = B$ the functions $\psi_{j,k}$ are known as a tight frame. For more information see Daubechies [1]. The inverse wavelet reconstruction method makes use of wavelet bases and frames, as well as the CWT.

Much of the present paper focuses on wavelets which are known to have what is known as a multiresolution analysis. A scaling function, sometimes called a father wavelet, is function $\phi(x)$ which satisfies the two-scale relations:

$$\phi(x) = \sum_{l=-\infty}^{\infty} h_l \phi(2x - l)$$

and

$$\psi(x) = \sum_{l=-\infty}^{\infty} g_l \phi(2x - l).$$

The functions $\phi_{m,l}(x) = 2^{m/2}\phi(2^m x - l)$ are orthonormal to each other and they are also orthonormal to $\psi_{m,l}(x) = 2^{m/2}\psi(2^m x - l)$. The functions ϕ and ψ allow for a decomposition of a function into the sum of a coarse approximation and finer details as follows:

$$f(x) = \sum_{l=-\infty}^{\infty} c_{M_0,l}\phi_{M_0,l}(x) + \sum_{m=M_0}^{\infty}\sum_{l=-\infty}^{\infty} d_{m,l}\psi_{m,l}(x)$$

which is truncated as

$$f_{M,L}(x) \simeq \sum_{l=-L}^{L} c_{M_0,l}\phi_{M_0,l}(x) + \sum_{m=M_0}^{M-1}\sum_{l=-L}^{L} d_{m,l}\psi_{m,l}(x).$$

The $c_{M_0,l}$ are known as approximation coefficients for the function at resolution scale M_0 and the $d_{m,l}$ are detail coefficients for the finer scales. This particular decomposition of a function into trend and details is known as a multiresolution analysis.

2 The Multiresolution Inverse Wavelet Reconstruction Method

2.1 Inverse Wavelet Reconstruction

We begin with a Fourier partial sum and assume that the function $f(x)$ can also be expressed as a discrete wavelet series:

$$f(x) = \sum_{m=-\infty}^{\infty}\sum_{l=-\infty}^{\infty} d_{m,l}\psi_{m,l}(x)$$

where

$$d_{m,l} = \int_{-\infty}^{\infty} f(x)\,\overline{\psi_{m,l}(x)}dx$$

and

$$\psi_{m,l}(x) = a_0^{-m/2}\psi(a_0^m x - b_0 l).$$

We now derive a formula expressing the Fourier coefficients in terms of wavelet coefficients.

$$\begin{aligned}
\widehat{f}(n) &= \frac{1}{2}\int_{-1}^{1} f(x)\,e^{-i\pi nx}dx \\
&= \frac{1}{2}\int_{-1}^{1}\sum_{m=-\infty}^{\infty}\sum_{l=-\infty}^{\infty} d_{m,l}\psi_{m,l}(x)\,e^{-i\pi nx}dx \\
&= \sum_{m=-\infty}^{\infty}\sum_{l=-\infty}^{\infty} d_{m,l}\left(\frac{1}{2}\int_{-1}^{1}\psi_{m,l}(x)\,e^{-i\pi nx}dx\right) \\
&= \sum_{m=-\infty}^{\infty}\sum_{l=-\infty}^{\infty} d_{m,l}\widehat{\psi}_{m,l}(n) \qquad (5)
\end{aligned}$$

The inverse wavelet reconstruction method is obtained by truncating the doubly infinite sum described above and solving for the wavelet coefficients. We suggest solving the following system of equations.

$$\widehat{f}(n) = \sum_{m=-M}^{M} \sum_{l=-L}^{L} d_{m,l} \widehat{\psi}_{m,l}(n) \tag{6}$$

for the wavelet coefficients $d_{m,l}$ where $n = -N...N$ and $N = 2ML + M + L$. One then computes the IWR approximation

$$S_{M,L} f(x) = \sum_{m=-M}^{M} \sum_{l=-L}^{L} d_{m,l} \psi_{m,l}(x). \tag{7}$$

The terms $\widehat{\psi}_{m,l}(n)$ are the nth Fourier coefficients of $\psi_{m,l}(x)$. Since we are solving a system of $2N+1$ equations in $(2M+1)(2L+1)$ unknown wavelet coefficients, in order for the system to be invertible we must have $2N+1 = (2M+1)(2L+1)$, or $N = 2ML + M + L$. Numerical experiments indicate that the invertibility condition can be relaxed and fewer wavelet coefficients can be computed if one solves the overdetermined system in a least squares sense using Matlab's backslash operator. This reconstruction is valid for both crude and non-crude wavelets.

2.2 Multiresolution IWR: Wavelet and Scaling Function Approach

Here we describe the IWR method for wavelets which allow for a multiresolution reconstruction. A formal derivation of the method proceeds again as follows. Write

$$\begin{aligned}
\widehat{f}(n) &= \frac{1}{2}\int_{-1}^{1} f(x)\, e^{-i\pi n x} dx \\
&= \frac{1}{2}\int_{-1}^{1} \left(\sum_{l=-\infty}^{\infty} c_{M_0,l} \phi_{M_0,l}(x) + \sum_{m=M_0}^{\infty} \sum_{l=-\infty}^{\infty} d_{m,l} \psi_{m,l}(x) \right) e^{-i\pi n x} dx \\
&= \sum_{l=-\infty}^{\infty} c_{M_0,l} \left(\frac{1}{2}\int_{-1}^{1} \phi_{M_0,l}(x)\, e^{-i\pi n x} dx \right) \\
&\quad + \sum_{m=M_0}^{\infty} \sum_{l=-\infty}^{\infty} d_{m,l} \left(\frac{1}{2}\int_{-1}^{1} \psi_{m,l}(x)\, e^{-i\pi n x} dx \right) \\
&= \sum_{l=-\infty}^{\infty} c_{M_0,l} \widehat{\phi}_{M_0,l}(n) + \sum_{m=M_0}^{\infty} \sum_{l=-\infty}^{\infty} c_{m,l} \widehat{\psi}_{m,l}(n)
\end{aligned} \tag{8}$$

The IWR method in this case is obtained by truncating the sums and solving the system of equations for the approximation and detail coefficients

$$\widehat{f}(n) = \sum_{l=-L}^{L} c_{M_0,l}\widehat{\phi}_{M_0,l}(n) + \sum_{m=M_0}^{M-1}\sum_{l=-L}^{L} d_{m,l}\widehat{\psi}_{m,l}(n) \tag{9}$$

where $n = -N...N$. Numerical results again indicate that the system can be solved in a least squares sense and one need not be concerned with meeting an invertibility condition exactly. One then constructs the multiresolution IWR approximation

$$S_{M,L}^{M_0} f(x) = A_L^{M_0}(x) + D_{M,L}^{M_0}(x)$$

where the coarse trend is given by

$$A_L^{M_0}(x) = \sum_{l=-L}^{L} c_{M_0,l}\phi_{M_0,l}(x)$$

and the finer details are given by

$$D_{M,L}^{M_0}(x) = \sum_{m=M_0}^{M-1}\sum_{l=-L}^{L} d_{m,l}\psi_{m,l}(x).$$

2.3 Multiresolution IWR: Pure Wavelet Approach

Next we describe an alternative multiresolution reconstruction for non-crude wavelets which does not make explicit use of the scaling function ϕ. It is simply a modification of the original IWR approximation. We write

$$S_{M,L}^{M_0} f(x) = A_{M,L}^{M_0}(x) + D_{M,L}^{M_0}(x)$$

where the coarse trend is given by

$$A_{M,L}^{M_0}(x) = \sum_{m=-M}^{M_0-1}\sum_{l=-L}^{L} d_{m,l}\psi_{m,l}(x)$$

and the finer details are given by

$$D_{M,L}^{M_0}(x) = \sum_{m=M_0}^{M}\sum_{l=-L}^{L} d_{m,l}\psi_{m,l}(x).$$

The derivation is simply to begin with the original IWR reconstruction and write

$$\begin{aligned} S_{M,L} f(x) &= \sum_{m=-M}^{M}\sum_{l=-L}^{L} d_{m,l}\psi_{m,l}(x) \\ &= \sum_{m=-M}^{M_0-1}\sum_{l=-L}^{L} d_{m,l}\psi_{m,l}(x) + \sum_{m=M_0}^{M}\sum_{l=-L}^{L} d_{m,l}\psi_{m,l}(x) \\ &= A_{M,L}^{M_0}(x) + D_{M,L}^{M_0}(x) \end{aligned}$$

The Pure Wavelet Approach will only provide a good decomposition into trend and details for wavelets which admit a scaling function, even though the method does not make explicit use of the scaling function. This is because the two approaches are approximately equivalent, that is:

$$A_L^{M_0}(x) \simeq A_{M,L}^{M_0}(x).$$

In fact,

$$A_L^{M_0}(x) = \sum_{l=-L}^{L} c_{M_0,l}\phi_{M_0,l}(x)$$

but also

$$\begin{aligned} A_L^{M_0}(x) &= \sum_{m=-\infty}^{M_0-1}\sum_{l=-L}^{L} d_{m,l}\psi_{m,l}(x) \\ &= \sum_{m=-\infty}^{-M-1}\sum_{l=-L}^{L} d_{m,l}\psi_{m,l}(x) + \sum_{m=-M}^{M_0-1}\sum_{l=-L}^{L} d_{m,l}\psi_{m,l}(x) \\ &= A_L^{-M}(x) + A_{M,L}^{M_0}(x). \end{aligned}$$

Since $A_L^{-M}(x)$ is the tail of a convergent series, $A_L^{-M}(x) \to 0$ as $M \to \infty$ since

3 A Version of IWR Based on the Continuous Wavelet Transform

Finally, we describe here a related method for implementing IWR which is based on a quadrature discretization of the inverse continuous wavelet transform. It produces results which are comparable to the standard wavelet series approach described previously. Our chief reason for considering it is allows us to consider any wavelet family as a candidate for use in reconstruction.

The derivation is as follows.

$$\begin{aligned} \widehat{f}(n) &= \frac{1}{2}\int_{-1}^{1} f(x)\, e^{-i\pi nx} dx \\ &= \frac{1}{2}\int_{-1}^{1}\left(\frac{1}{C_\psi}\int_{-\infty}^{\infty}\int_{-\infty}^{\infty}\frac{F_\psi(b,a)}{a^2}\psi\left(\frac{x-b}{a}\right)dadb\right)e^{-i\pi nx}dx \\ &= \frac{1}{C_\psi}\int_{-\infty}^{\infty}\int_{-\infty}^{\infty}\frac{F_\psi(b,a)}{a^2}\left(\frac{1}{2}\int_{-1}^{1}\psi\left(\frac{x-b}{a}\right)e^{-i\pi nx}dx\right)dadb \\ &= \int_{-\infty}^{\infty}\int_{-\infty}^{\infty}\frac{1}{C_\psi}\frac{F_\psi(b,a)}{a^2}\widehat{\psi}_{b,a}(n)\, dadb. \end{aligned} \tag{10}$$

Note that in this section we use $\widehat{\psi}_{b,a}(n)$ to denote the nth Fourier coefficient of $\psi\left(\frac{x-b}{a}\right)$.

Truncate the limits of integration and write

$$\widehat{f}(n) \simeq \int_{-B}^{B}\int_{-A}^{A} \frac{1}{C_\psi}\frac{F_\psi(b,a)}{a^2}\widehat{\psi}_{b,a}(n)\,dadb. \tag{11}$$

Next, discretize the integrations using a quadrature rule such as the trapezoidal rule or Gauss quadrature. The resulting equations become

$$\widehat{f}(n) \simeq \sum_{l=0}^{L}\sum_{m=0}^{M} \frac{1}{C_\psi}\frac{F_\psi(b_l,a_m)}{a_m^2}\widehat{\psi}_{b_l,a_l}(n) \tag{12}$$

which can be expressed in simpler form by letting $d_{m,l} = \frac{1}{C_\psi}\frac{F_\psi(b_l,a_m)}{a_m^2}$ and writing

$$\widehat{f}(n) \simeq \sum_{m=0}^{M}\sum_{l=0}^{L} d_{m,l}\widehat{\psi}_{b_l,a_l}(n). \tag{13}$$

Finally, solve the system of equations, possibly in a least squares sense, for the coefficients $d_{m,l}$ and construct the nonstandard wavelet series approximation:

$$f(x) \simeq \sum_{m=0}^{M}\sum_{l=0}^{L} d_{m,l}\psi\left(\frac{x-b_l}{a_m}\right). \tag{14}$$

4 Numerical Results

Numerical experiments show that the IWR method based on a quadrature discretization of the CWT yields uniformly converging approximations for all wavelet families we have tested. We display the results of the Haar, Shannon, and Mexican hat wavelets in the figures below. The Haar and Shannon systems are some of the earliest examples of what later became wavelets. The Haar wavelet is apparently able to resolve an interior discontinuity without prior knowledge as to its location, as well as the endpoints. Therefore the Haar wavelet is able to provide a global reconstruction, albeit a low order accuracy one. The low order of convergence is due to the fact that the wavelet is not well-localized in Fourier space. Shannon wavelets will resolve the Gibbs phenomenon at the endpoints of the interval and Mexican hat wavelets will do it even better.

Numerical experiments also show that the Multiresolution IWR method is able to decompose a function into a course trend plus finer details, given a function's Fourier coefficients. We provide numerical examples using the both the Pure Wavelet Approach to reconstruction and the Wavelet and Scaling function Approach described above. We implemented the inverse wavelet reconstruction method by computing Fourier coefficients for the test functions in question using trapezoidal rule quadrature. This makes our Fourier series a pseudospectral series. For the method to be accurate we compute the coefficients $\widehat{\psi}_{m,l}(n)$ using the same trapezoidal rule quadrature.

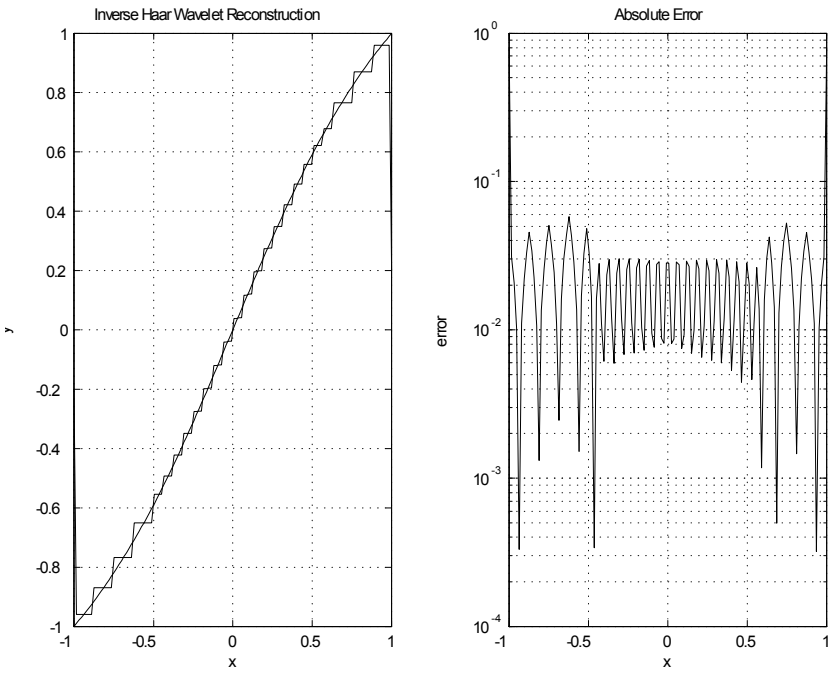

Figure 1: Inverse Haar Reconstruction of $\frac{4}{\pi}\tan^{-1}x$ based on 64 Fourier coefficients using the wavelet series approach.

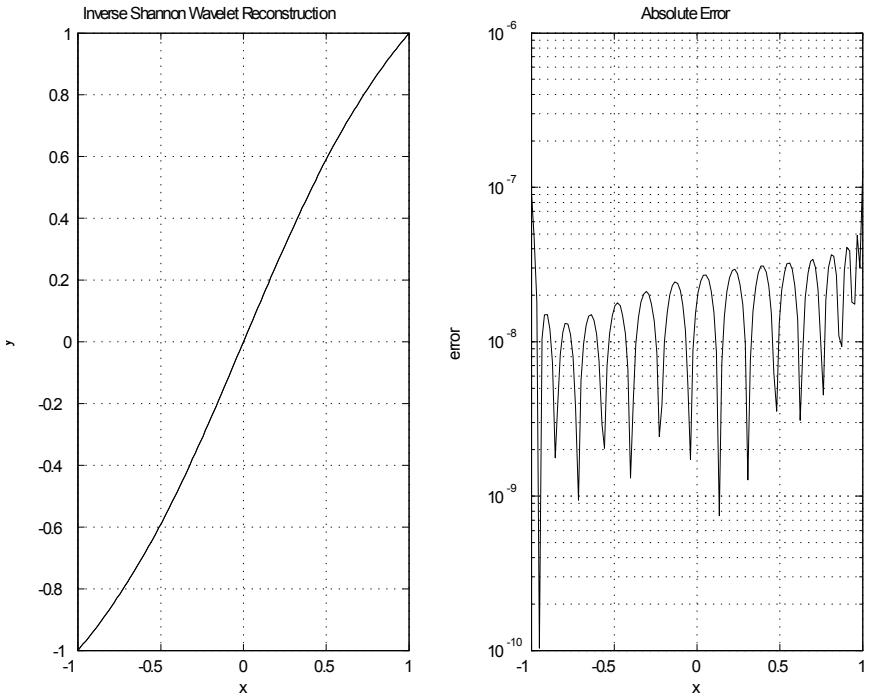

Figure 2: Inverse Shannon reconstruction of $\frac{4}{\pi}\tan^{-1} x$ using the CWT approach from 128 Fourier coefficients. The limits of integration are $A = B = 20$ and 64 Gauss-Legendre quadrature nodes in a and b are employed.

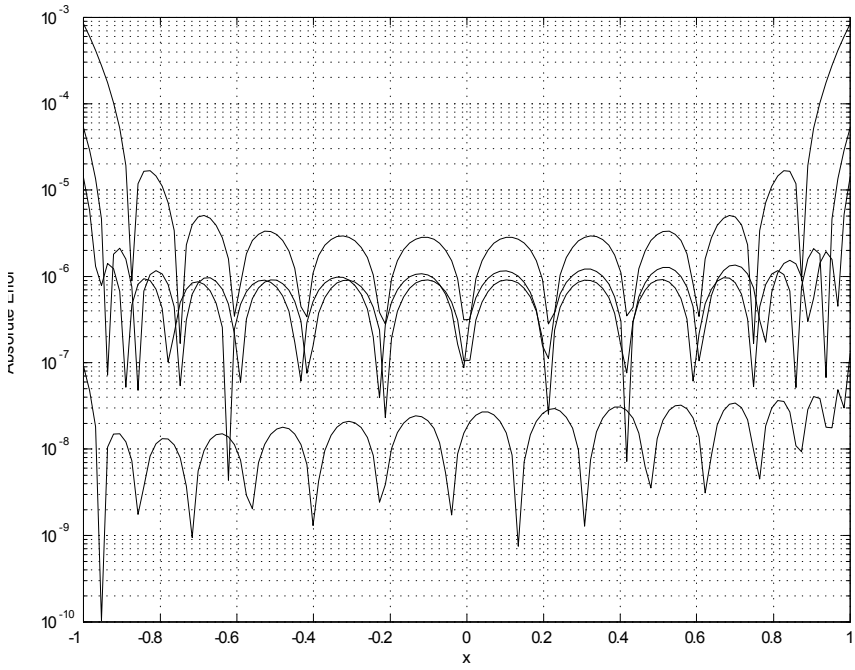

Figure 3: Converge of Inverse Shannon reconstruction of $\frac{4}{\pi}\tan^{-1} x$ using the CWT approach from 16, 32, 64, and 128 Fourier coefficients. The limits of integration are $A = B = 20$ and the number of Gauss-Legendre quadrature nodes in a and b are equal to the number of Fourier coefficients.

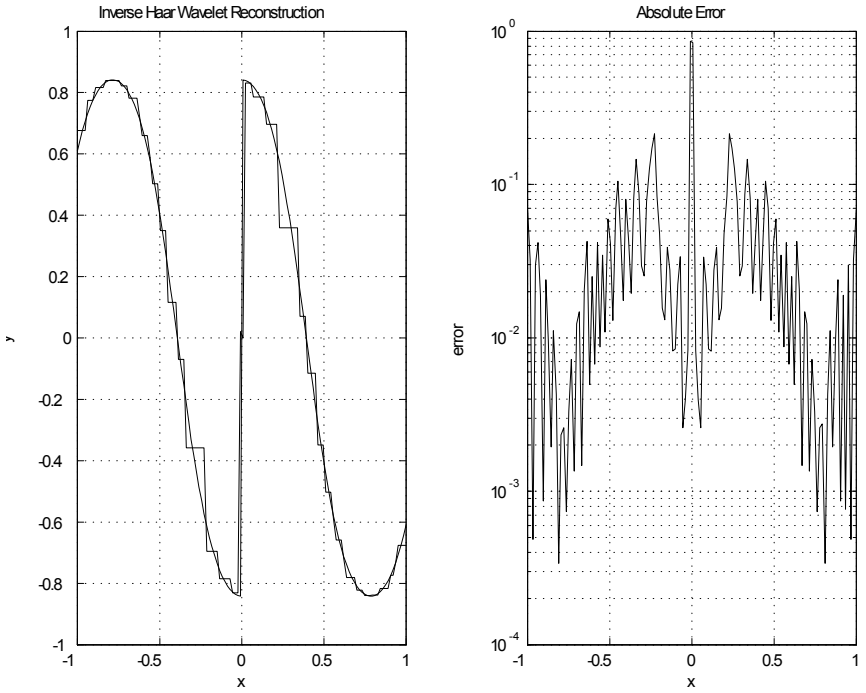

Figure 4: Inverse Haar reconstruction of $\sin(\cos(4x))\,\mathrm{sgn}(x)$ utlilizing the CWT approach with $A = B = 20$, and Gauss-Legendre quadrature with 32 quadrature nodes in a and 32 quadrature nodes in b. The method resolves both endpoint and interior discontinuties, albeit with low accuracy.

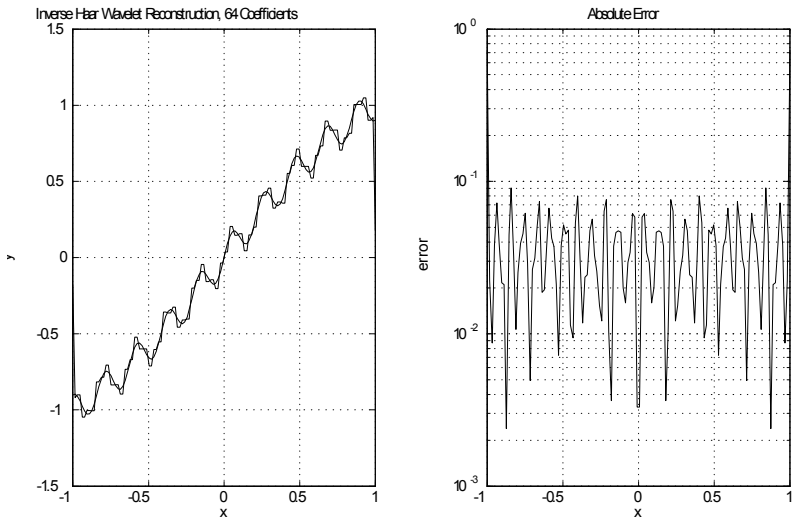

Figure 5: Inverse Haar wavelet reconstruction using the pure wavelet approach of the function $f(x) = \frac{4}{\pi}\tan^{-1} x + \frac{1}{10}\sin 30x$ based on 64 Fourier coefficients.

We consider the test function $f(x) = \frac{4}{\pi}\tan^{-1}(x) + \frac{1}{10}\sin(30x)$ to observe the ability of various wavelets to extract the trend, mostly due to $\tan^{-1}(x)$, and smaller scale oscillations due to $\frac{1}{10}\sin(30x)$. We display here the results of the Haar wavelet: the simplest wavelet which admits a multiresolution analysis. We also consider the piecewise linear Franklin wavelets generated by the second order splines.

5 Conclusions

Numerical results indicate that the IWR method based on the continuous wavelet transform works as well as the IWR method based on a standard wavelet series. It yields an accurate and rapidly converging approximation. The multiresolution IWR methods allows one to separate out from the Fourier coefficients a course trend and finer details regardless of any Gibbs phenomenon. Work in progress includes a numerical study of the multiresolution IWR method for a wider variety of wavelets, multiresolution reconstruction from series other than Fourier series, a two-dimensional implementation and a proof of convergence.

References

[1] I. Daubechies, Ten Lectures on Wavelets, CBMS-NSF Regional Conference Series in Applied Mathematics, SIAM, Philadelphia, 1992.

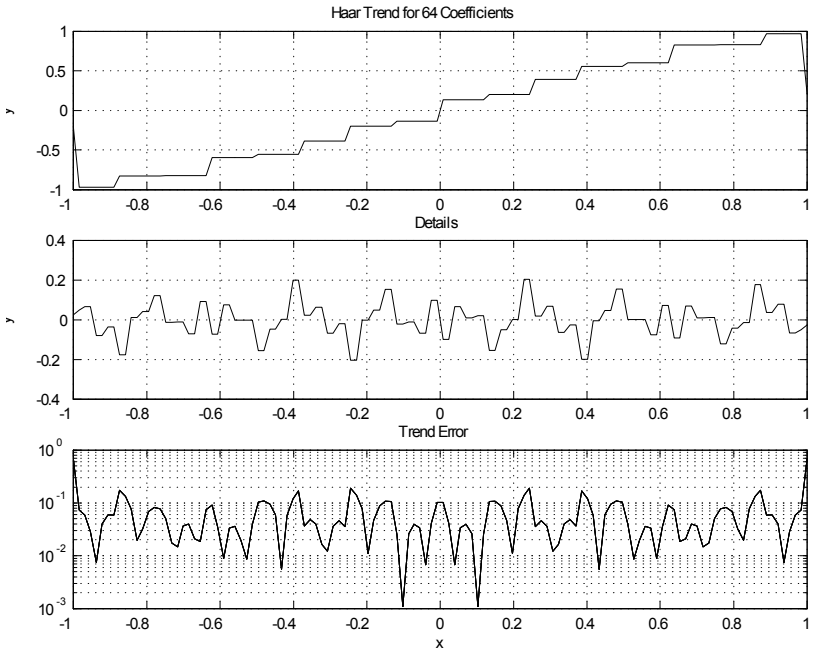

Figure 6: Inverse Haar decomposition of $f(x) = \frac{4}{\pi}\tan^{-1} x + \frac{1}{10}\sin 30x$ into a trend and details using the pure wavelet approach.

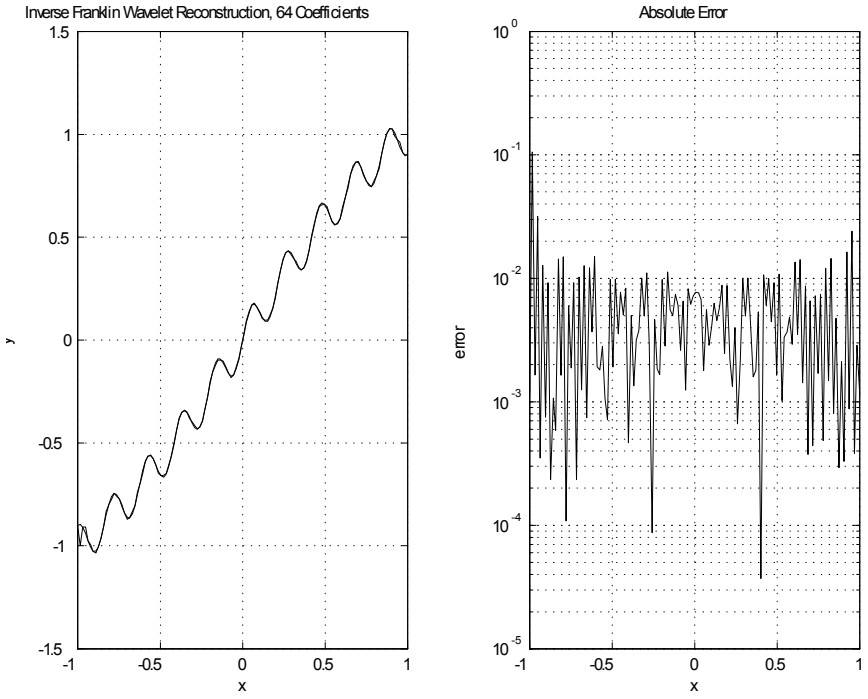
Inverse Franklin Wavelet Reconstruction, 64 Coefficients
y
x
1.5
1
0.5
0
-0.5
-1
-1.5
-1
-0.5
0
0.5
1
Absolute Error
error
x
10^{0}
10^{-1}
10^{-2}
10^{-3}
10^{-4}
10^{-5}
-1
-0.5
0
0.5
1

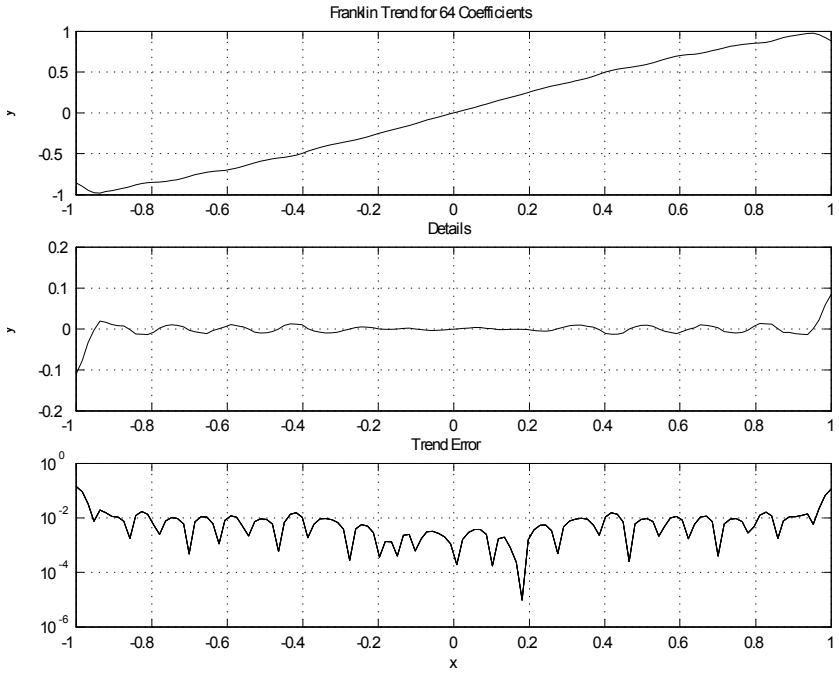

Figure 7: Inverse Franklin decomposition of $f(x) = \frac{4}{\pi}\tan^{-1} x + \frac{1}{10}\sin 30x$ into a trend and details.

[2] T. A. Driscoll, and B. Fornberg, A Pade-based Algorithm for Overcoming the Gibbs Phenomenon, *Numerical Algorithms,* 26, 2001, pp. 77-92.

[3] A. Gelb, and E. Tadmor, Detection of Edges in Spectral Data, *Appl. Comp. Harmonic Anal.*, 7, 1999, pp. 101-135.

[4] A. Gelb, and E. Tadmor, Detection of Edges in Spectral Data II. Nonlinear Enhancement, *SIAM J. Numer. Anal.*, Vol. 38, No. 4, 2000, pp. 1389-1408.

[5] A. Gelb, and E. Tadmor, Spectral Reconstruction of Piecewise Smooth Functions from their Discrete Data, *Mathematical Modeling and Numerical Analysis*, 36:2, 2002, pp. 155-175.

[6] A. Gelb, and J. Tanner, Robust Reprojection Methods for the Resolution of the Gibbs Phenomenon., *Applied Computational and Harmonic Analysis*, Vol. 20, 1, 2006, pp. 3-25.

[7] D. Gottlieb, C.-W. Shu, A. Solomonoff, and H. Vandeven, On the Gibbs's Phenomenon I: Recovering Exponential Accuracy from the Fourier Partial Sum of a Nonperiodic Analytic Function, *J. Comput. Appl. Math.*, 43, 1992, pp. 81-92 .

[8] D. Gottlieb, and E. Tadmor, Recovering Pointwise Values of Discontinuous Data within Spectral Accuracy, in: *Progress and Supercomputing in Computational Fluid Dynamics*, Proceedings of a 1984 U.S.-Israel Workshop, Progress in Scientific Computing, Vol. 6 (E. M. Murman and S. S. Abarbanel eds.), Birkhauser, Boston, 1985, pp. 357-375.

[9] D. Gottlieb and C.-W. Shu, On the Gibbs Phenomenon and its Resolution, *SIAM Rev.*, Vol. 39, 1997, pp. 644-668.

[10] N. Greene, *On the Recovery of Piecewise Smooth Functions from their Integral Transforms and Spectral Data*, Ph.D. Dissertation, SUNY Stony Brook, 2004.

[11] N. Greene, A Wavelet-based Method for Overcoming the Gibbs Phenomenon, in: *Recent Advances on Applied Mathematics: Proceedings of the American Conference on Applied Mathematics*, Cambridge, Massachusetts, March 24-26, 2008, pp. 408-412.

[12] N. Greene, Inverse Wavelet Reconstruction for Resolving the Gibbs Phenomenon, International Journal of Circuits, Systems and Signal Processing, Issue 2, Vol. 2, 2008, pp. 73-77.

[13] J.-H. Jung, and B. D. Shizgal, Generalization of the Inverse Polynomial Reconstruction Method in the Resolution of the Gibbs Phenomenon, *J. Comp. Appl. Math.*, v. 172, n.1, 2004, pp.131-151.

[14] J.-H. Jung, and B. D. Shizgal, Inverse polynomial reconstruction of two dimensional Fourier images, *J. Scientific Computing*, v.25, n.3, 2005, pp. 367-399.

[15] J.-H. Jung, and B. D. Shizgal, On the numerical convergence with the inverse polynomial reconstruction method for the resolution of the Gibbs phenomenon, *J. Computational Physics*, 224, 2007, pp. 477-488.

[16] B. D. Shizgal and J.-H. Jung, Towards the resolution of the Gibbs Phenomena, *J. Comput. Appl. Math.*, 16, 2003, pp. 41-65.

[17] R. Pasquetti, On Inverse methods for the Resolution of the Gibbs Phenomenon, *Journal of Computational and Applied Mathematics*, Vol. 170, no. 2, 2004, pp. 305-315.

[18] E. Tadmor and J. Tanner, Adaptive Mollifiers - High Resolution Recovery of Piecewise Smooth Data from its Spectral Information, *J. Foundations of Comp. Math.* 2, 2002, 155-189.

[19] E. Tadmor and J. Tanner, Adaptive Filters for Piecewise Smooth Spectral Data, *IMA J. Numerical Anal.*, Vol. 25, 4, 2005, pp. 635-647.